CRYSTAL GROWTH & DESIGN

ARTICLE

pubs.acs.org/crystal

Sulfonamide−Pyridine-N-oxide Cocrystals

N. Rajesh Goud, N. Jagadeesh Babu, and Ashwini Nangia*

School of Chemistry, University of Hyderabad, Prof. C. R. Rao Road, Gachibowli, Hyderabad 500 046, India

Supporting Information

ABSTRACT: Hydrogen-bond motifs for the supramolecular synthesis of sulfonamide−pyridine-N-oxide complexes were derived from the analysis of cocrystal structures of aryl sulfonamides and pyridine-N-oxides. The sulfonamide NH donor persistently interacts with the N-oxide acceptor via a N−H···O hydrogen bond, though the exact geometry of the motif, such as discrete (D), infinite chain C(4), cyclic motifs $R_4^2(8)$ or $R_2^2(4)$, varies from structure to structure. Surprisingly, the two-point $R_2^2(8)$ cyclic motif of N−H···O and C−H···O hydrogen bonds, analogous to the heterosynthon in carboxamide−pyridine-N-oxide cocrystals, was not observed in sulfonamide−N-oxide cocrystals. The utility of this model study is demonstrated by making cocrystals of Furosemide with 4,4′-bipyridine-N,N′-dioxide and isonicotinamide-N-oxide.

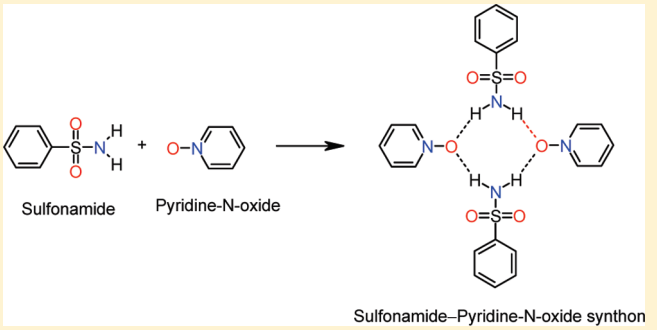

INTRODUCTION

The identification of new and robust supramolecular synthons is the first step in the crystal engineering of organic solids. Following up on Desiraju's[1] supramolecular synthon concept, Zaworotko[2] subclassified synthons as heterosynthons (those between complementary unlike functional groups) and homosynthons (between the same functional group). Some common examples of homo- and heterosynthons and their probability statistics[3] in the Cambridge Structural Database[4] are given in Scheme 1. Ideally, one would like to find out the likelihood of a particular synthon for retrosynthetic planning.[5] Cyclic synthons, or hydrogen bond ring motifs, can be classified according to the graph set notation[6] as $R_4^2(8)$, $R_2^2(7)$, etc. Etter's[7] hydrogen bond rules guide the pairing-off of donors and acceptors in a multifunctional system: the best donor in the molecule preferentially interacts with the best acceptor in the system, the second best donor−acceptor group hydrogen bond next, and so on. For example, in carboxylic acid−carboxamide heterosynthon, the strongest donor (COOH) hydrogen bonds to the best acceptor (amide C═O) and then the next best donor−acceptor, amide NH and acid C═O, pair up to give the $R_2^2(8)$ motif of 47% occurrence probability.[8] Similarly, acid−pyridine heterosynthon of $R_2^2(7)$ graph set is the most popular supramolecular synthon in the crystal engineer's toolkit with >90% success rate.[9]

Some time ago we noted that the carboxamide functional group does not have an equivalent high-probability motif, and developed the novel carboxamide−pyridine-N-oxide heterosynthon of $R_2^2(8)$ geometry.[10] The strong amide NH to N-oxide N−H···O motif has a good occurrence probability of 70% compared to 4% for amide−pyridine. Carboxylic acids and carboxamide are the most popular organic functional groups for crystal design and they are often found in pharmaceutical molecules.[11] The sulfonamide group occupies a place of prominence in drug molecules, being the common functional moiety of sulfa drugs.[12] Whereas a few isolated cases of sulfonamide hydrogen bonding to other functional groups, such as COOH, $CONH_2$, urea, etc., are reported[13] there is no specific heterosynthon associated with the SO_2NH_2 group. Sulfoxide as a potent cocrystal former for the NH functional group via a N−H···O═S hydrogen bond was recently reported.[14] Our

Scheme 1. Strong Hydrogen-Bond Homosynthons and Heterosynthons with Their Occurrence Probability Indicated

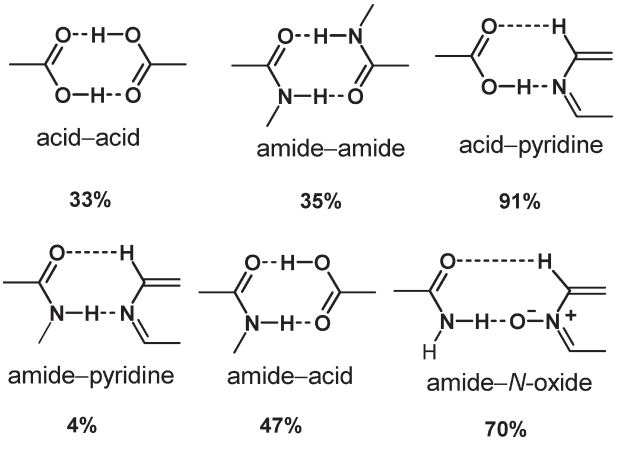

Received: January 22, 2011
Revised: March 5, 2011
Published: March 10, 2011

Scheme 2. Homo- vs Heterosynthon Competition for the Sulfonamide Group[a]

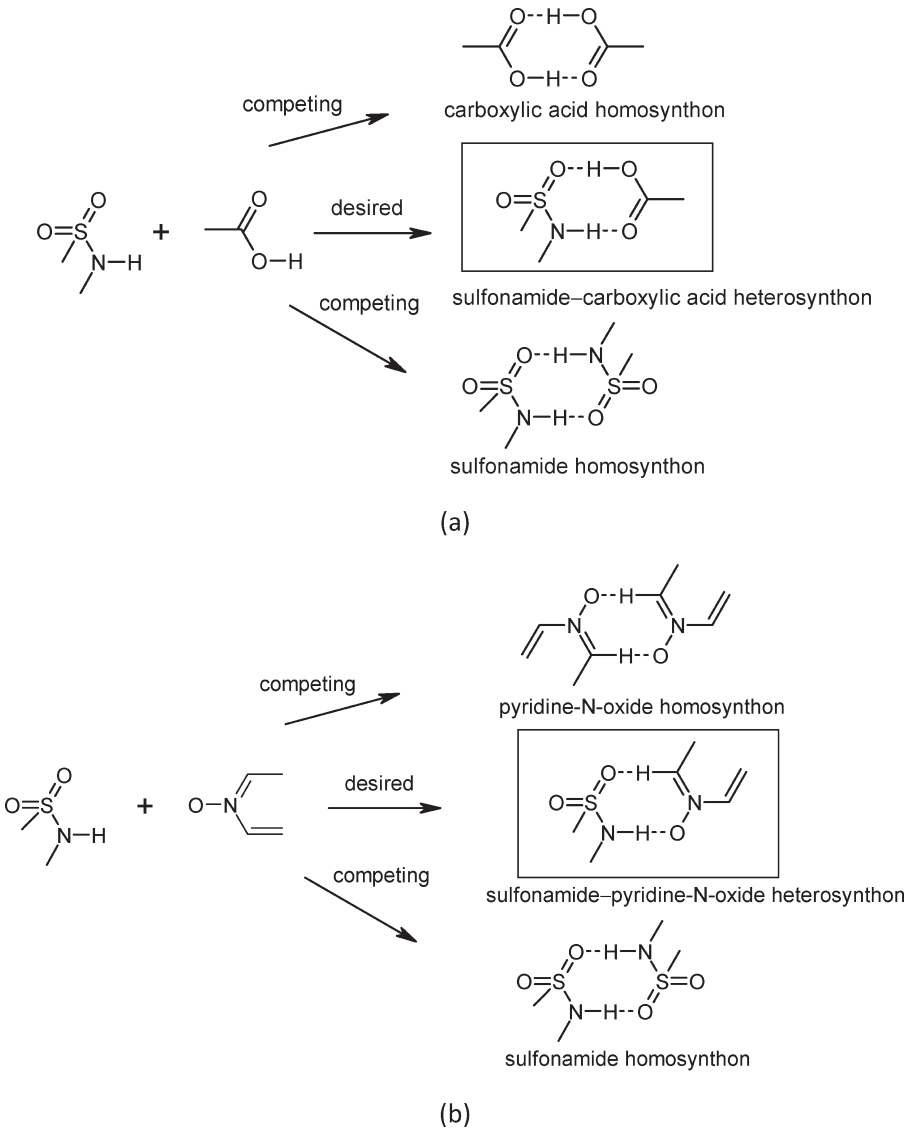

[a] (a) In sulfonamide−COOH (or $CONH_2$), the hydrogen bonds are of the strong O−H···O/N−H···O type in the target heterosynthon and the competing homosynthons. (b) In sulfonamide−pyridine-N-oxide, the target sulfonamide−pyridine-N-oxide has strongest donor−strongest acceptor pairing, whereas the competing homosynthons are not so strong. This should give a higher success rate for the sulfonamide group to hydrogen bond with pyridine-N-oxide in co-crystallization experiments.

objective was to use pyridine-N-oxide as complementary hydrogen bond acceptor for the SO_2NH_2 group. An advantage with pyridine-N-oxide compared to COOH and $CONH_2$ as a complementary functional group is that homosynthon competition is minimal because the pyridine-N-oxide lacks strong donor groups of its own (Scheme 2).

A stable heterosynthon assembly is based on the fact that the dissimilar functional groups will aggregate better compared to identical ones. Observations such as (1) the carboxamide−pyridine-N-oxide heterosynthon has hydrogen bond strength greater than the constituent homosynthons by about 3 kcal/mol,[10] and (2) that pyridine-N-oxides are able to disrupt the strong urea α-network[15] suggested that the pyridine-N-oxide group will be a good complementary partner for the sulfonamide group to prepare heteromeric cocrystals (Scheme 3).

RESULTS

A search of the CSD[4] (August 2010 update) for the sulfonamide group with the filters '3D coordinates determined, R-factor <0.1, organic molecules only' gave 2090 hits, which included primary and secondary sulfonamide structures. This sulfonamide subdatabase contained only 34 cocrystals without any solvent/water inclusion, of which 6 are with primary sulfonamides. There are 75 multicomponent complexes such as salt hydrates and cocrystal solvates, 165 solvates, and 61 salt structures. The propensity of sulfonamide to form cocrystals is 1.63%, molecular complexes 3.59%, solvates 7.89%, and salts 2.91%. This means that the sulfonamide functional group is relatively less explored for cocrystal engineering. Moreover, the current version of the Cambridge database does not contain even a single hit of a primary sulfonamide and pyridine N-oxide

Scheme 3. Primary Sulfonamide and Pyridine-N-oxide coformers Gave Five Cocrystals and a Quarter Hydrate As Listed above (abbreviations are used throughout the paper)

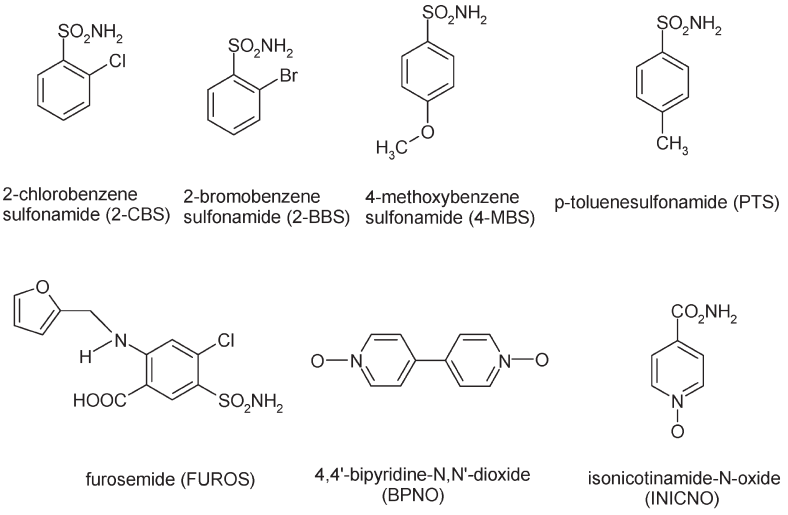

2-CBS–BPNO (1:1)	2-BBS–BPNO (1:0.5)	4-MBS–BPNO (1:0.5)
PTS–BPNO (2:1)	FUROS–BPNO–H_2O (1:1:0.25)	FUROS–INICNO (1:1)

functional group in the same crystal structure, suggesting that this class of heteromeric cocrystals is completely unexplored. We report six novel cocrystals of a few model sulfonamides and a well-known drug molecule Furosemide (Lasix) with pyridine-N-oxides as coformers. The objective was to understand the nature of hydrogen bonding in cocrystal structures and to know if a particular motif is strong and recurring to be reliably used for crystal design.

The most common method of obtaining cocrystals is to dissolve the components in a suitable solvent for single crystals of the binary phase to appear after slow evaporation of solvent(s). Gentle warming is necessary to dissolve the solids, and an antisolvent is added to accelerate crystallization. This empirical, trial-and-error method, referred to as solution crystallization, was repeated with several solvents until there was evidence of a new chemical complex or cocrystal based on DSC, IR, powder X-ray diffraction, and single-crystal X-ray structure. Precipitation of the individual components instead of the desired cocrystal and formation of undesired solvates/hydrates are common difficulties in the solution-based approach. Solid-state grinding[16] overcomes the problem of solvent inclusion, but the product is usually microcrystalline for routine single-crystal X-ray structure determination. Adding a few drops of solvent during grinding/kneading, referred to as liquid-assisted grinding,[17] accelerates cocrystal formation due to lubrication.

Cocrystals of 2-CBS, 4-MBS, 2-BBS, and PTS were obtained by the traditional solution crystallization method (see Scheme 3 for chemical diagrams). However, this method was not successful with FUROS. Liquid-assisted grinding with acetonitrile solvent gave 0.25 hydrate with BPNO and a cocrystal with INICNO (see Scheme 3 for chemical diagrams and Experimental Section for cocrystallization details). The molecular stoichiometry and composition of each cocrystal was confirmed from its X-ray crystal structure. Attempts with increasing the temperature of the solid-state reaction[18] or melt cocrystallization[19] did not yield any new adduct. Crystallographic parameters and hydrogen bond metrics are listed in Table 1 and Table 2. Since both S═O and N-oxide acceptors are present in the system, the O atom is subscripted to identify the functional group as $O_{sulfonamide}$ or O_{Noxide} whenever there is ambiguity.

Crystal Structure Analysis. *2-Chlorobenzene Sulfonamide—Bipyridine-N,N′-dioxide (2-CBS:BPNO 1:1).* This crystal structure in tetragonal space group $P4_32_12$ contains one molecule each of 2-CBS and BPNO in the asymmetric unit. The 2-CBS and BPNO molecules form a zigzag tape along the crystallographic [001] axis via a N—H···O_{Noxide} hydrogen bond (1.80 Å, 173°). The normal sulfonamide dimer of N—H···$O_{sulfonamide}$ is absent; one of the sulfonamide O is involved in intramolecular C—Cl···O contact of 3.06 Å.[20] The cocrystal units are connected through C—H···O_{Noxide} interactions of BPNO (Figure 1).

2-Bromobenzene Sulfonamide—Bipyridine-N,N′-dioxide (2-BBS:BPNO 1:0.5). 2-BBS and BPNO molecules form a two-dimensional array of tetrameric ring motif $R_4^2(8)$ of N—H···O_{Noxide} hydrogen bonds. There are auxiliary O···Br interactions in a 10-member ring as shown in Figure 2. Thus while 2-CBS has single N—H···O_{Noxide} hydrogen bond, BBS makes a ring motif with the coformer.

4-Methoxybenzene Sulfonamide—bipyridine-N,N′-dioxide (4-MBS:BPNO 1:0.5). 4-MBS molecules form a linear tape along the [010] axis through one point N—H···O_{Noxide} and N—H···$O_{sulfonamide}$ hydrogen bond (1.99 Å, 166°; 1.74 Å, 167°). Four 4-MBS and 2 BPNO molecules make large $R_6^6(24)$ rings with the p-anisyl groups projecting above and below the ring plane (Figure 3). The commonly occurring sulfonamide dimer is absent in this structure. There is also an N—H···$O_{sulfonamide}$ C(4)chain that can be discerned in the structure.

4-Toluene Sulfonamide—bipyridine-N,N′-dioxide (PTS:BPNO 2:1). PTS and BPNO molecules form tetrameric ring motif $R_4^2(8)$of N—H···O_{Noxide} hydrogen bonds through two symmetry independent TS molecules and one BPNO (1.85 Å, 173°, 1.97 Å, 164°, 1.86 Å, 164°, 1.80 Å, 171°) as shown in Figure 5. The sulfonamide O atoms are engaged in $R_2^2(9)$ motif of C—H···O interactions (Figure 6).

Table 1. X-ray Crystal Structure Data

	2-CBS−BPNO (1:1)	2-BBS−BPNO (1:0.5)	4-MBS−BPNO (1:0.5)	PTS−BPNO (2:1)	FUROS−BPNO−H_2O (1:1:0.25)	FUROS−INICNO (1:1)
empirical formula	$(C_6H_6O_2NSCl)\cdot(C_{10}H_8N_2O_2)$	$(C_6H_6O_2NSBr)\cdot 0.5(C_{10}H_8N_2O_2)$	$(C_7H_9O_3NS)\cdot 0.5(C_{10}H_8N_2O_2)$	$2(C_7H_9O_2NS)\cdot(C_{10}H_8N_2O_2)$	$(C_{12}H_{11}O_5N_2ClS)\cdot(C_{10}H_8N_2O_2)\cdot 0.5(O)$[a]	$(C_{12}H_{11}O_5N_2ClS)\cdot(C_6H_6O_2N_2)$
fw	379.81	660.36	562.61	530.61	526.92	468.87
cryst syst	tetragonal	triclinic	monoclinic	monoclinic	triclinic	triclinic
space group	$P4_32_12$	$P\bar{1}$	$P2_1/c$	$P2_1/c$	$P\bar{1}$	$P\bar{1}$
T (K)	100(2)	298(2)	100(2)	100(2)	100(2)	100(2)
a (Å)	7.8871(5)	8.181(3)	8.7426(8)	10.3170(9)	8.0230(6)	5.2214(4)
b (Å)	7.8871(5)	8.421(3)	5.2061(5)	12.3913(10)	8.3201(6)	9.5860(8)
c (Å)	51.100(7)	10.250(4)	27.7269(19)	20.0553(17)	17.5479(12)	20.1540(17)
α (deg)	90.00	98.774(6)	90.00	90.00	77.7340(10)	85.2220(10)
β (deg)	90.00	95.521(6)	102.935(2)	103.7280(10)	77.5200(10)	88.7590(10)
γ (deg)	90.00	114.520(6)	90.00	90.00	81.2860(10)	74.8260(10)
Z	8	1	2	4	2	2
V (Å^3)	3178.7(5)	624.9(4)	1229.96(18)	2490.6(4)	1110.71(14)	970.20(14)
D_{calcd} (g cm^{-3})	1.587	1.755	1.519	1.415	1.576	1.605
no. of reflns collected	32933	6340	11917	25031	11547	10099
no. of obsd reflns	3142	2406	2422	4856	4339	3808
no. of unique reflns	3134	2207	2290	4493	4043	3566
R_1 [$I > 2\sigma(I)$]	0.0325	0.0299	0.0397	0.0335	0.0376	0.0317
wR_2 [all]	0.0781	0.0764	0.1036	0.0900	0.0973	0.0849
no. of params	234	163	173	343	341	338
GOF	1.150	1.110	1.082	1.017	1.059	1.038

[a] Water was assigned 0.25 sof in crystal structure. H atoms are omitted. SHELX refinement gave a value of 0.5(O).

Furosemide−Bipyridine-N,N′-dioxide−0.25Hydrate (FUROS−BPNO−H_2O 1:1:0.25). The presence of partial water occupancy in the crystal structure was initially suggested by unaccounted for electron density of about 1.67 Å^3 in the structure during refinement and checking cycles.[21] Placing a partial water at this site of 0.25 atom occupancy gave better structure convergence and R-factor. Hence the quarter hydrate stoichiometry is fixed for this cocrystal. The crystal structure contains a prominent tetrameric ring motif of graph set $R_2^2(4)$ connected through strong N−H···O_{Noxide} hydrogen bond (2.04 Å, 140.2°; Figure 7). The FUROS molecular conformation is frozen by an intramolecular N−H···O bond (1.91 Å, 132.3°) from the amine NH to the carboxylic acid C═O of S(6) notation. Two partial occupancy water molecules act as bridges to two N-oxide groups, which is chemically reasonable interaction geometry. Further, the loss of water could be detected in TGA (see Figure S1 in the Supporting Information). Incidentally, the structure contains the sulfonamide N−H···O dimer (1.95 Å, 153.2°) common in sulfonamide crystal structures (Figure 8). The $R_2^2(4)$ ring motifs are connected through O−H···O_{Noxide} (1.62 Å, 157.9°) shown in Figure 9.

Furosemide−Isonicotinamide-N-oxide (FUROS−INICNO 1:1). The FUROS molecule is disordered at the furan ring. The $R_2^2(8)$ ring motif between the carboxylic group of FUROS and the carboxamide group of INICNO is the main heterosynthon (N−H···O 1.87 Å, 167°; O−H···O 1.60 Å, 168°). The sulfonamide group connects FUROS to the N-oxide moiety on the other side (N−H···O_{Noxide} 1.80 Å, 162°) as shown in the Figure 10.

The FUROS and INICNO molecules extend to make a larger $R_4^4(32)$ [$R_2^2(8)$] ring motif, which in turn is connected through C−H···O $R_2^2(8)$ dimer as shown in Figure 11.

Vibrational Spectroscopic Characterization. All compounds were characterized by IR, Raman, and NIR spectroscopy and by changes in the signature peaks associated with the transformation of the sulfonamide and the coformer to the new cocrystal structure. The N−H stretching vibrations of the sulfonamide group showed the expected red shift of 10−40 cm^{-1} due the formation of the stronger N−H···O_{Noxide} hydrogen bond in the cocrystal compared to N−H···$O_{sulfonamide}$, i.e., the N−H bond is weaker in the cocrystal. This bathochromic shift is observed for all cocrystals (see Figure S2 in the Supporting Information). There are clear differences in the solid-state spectra of the starting components compared to that of the product cocrystals (see Table S1 in the Supporting Information).

Similar to the IR spectra, the Raman spectra showed bathochromic shift in the N−H stretching peaks due to the weakening of the N−H bond after stronger hydrogen bonding with the pyridine-N-oxide acceptor. However, due to the weak intensities of the Raman resonances the symmetric and asymmetric N−H peaks merged together to give a single broad band between 3400 and 3200 cm^{-1} in all the cocrystals and the hydrate (see Figure S3 in the Supporting Information). Attempts to resolve the N−H peaks by increasing the laser intensity invariably caused sample burn. The changes in the N−H stretch, bend and S═O stretch vibrations are listed in Table S2 in the Supporting Information.

NIR spectra were analyzed in the 4000−7000 cm^{-1} range. The N−H overtone vibrations at 6400−6200 cm^{-1} (see Figure S3 in the Supporting Information) are consistent with the fundamental N−H stretch resonances in the IR and Raman spectra wherein the bathochromic shift of about

Table 2. Hydrogen Bond Distance and Angle (neutron-normalized N−H, O−H, and C−H distance)

D−H···A	D···A (Å)	H···A (Å)	D−H···A (deg)	symmetry code
		2-CBS−BPNO (1:1)		
N1−H1A···O4	2.806(3)	1.80	172.9	1/2 + y, 1/2 − x, −3/4 + z
N1−H1B···O3	2.839(3)	1.87	158.0	1 + x, −1 + y, −1 + z
C3−H3···N1	3.388(3)	2.51	136.5	−1 + x, y, z
C5−H5···O1	3.497(3)	2.42	168.4	−1/2 + x, 1/2 − y, 1/4 − z
C6−H6···O1	2.825(3)	2.36	103.6	[a]
C8−H8···O3	3.428(3)	2.35	173.0	y, 1 + x, 2 − z
C12−H12···O4	3.360(3)	2.29	169.2	3/2 − x, 1/2 + y, 7/4 − z
C13−H13···O3	3.383(3)	2.40	149.1	y, 1 + x, 2 − z
C16−H16···O4	3.233(3)	2.23	153.1	3/2 − x, −1/2 + y, 7/4 − z
		2-BBS−BPNO (1:0.5)		
N1−H1A···O3	2.812(3)	2.00	135.6	1 − *x*, 1 − *y*, −*z*
N1−H1B···O3	2.806(3)	1.80	172.5	*x*, −1 + *y*, *z*
C2−H2···O2	3.108(3)	2.40	121.3	−1 − *x*, 1 − *y*, 2 − *z*
		4-MBS−BPNO (1:0.5)		
N1−H1A···O3	2.737(2)	1.74	166.7	*x*, −1 + *y*, *z*
N1−H2A···O2	2.988(2)	1.99	165.7	*x*, 1 + *y*, *z*
C12−H12···O1	3.321(2)	2.29	157.4	−1 + *x*, 1 + *y*, *z*
		PTS−BPNO (2:1)		
N2−H1A···O5	2.850(2)	1.86	164.0	−1 + *x*, *y*, *z*
N2−H2A···O6	2.809(2)	1.80	170.7	*x*, 3/2 − *y*, 1/2 + *z*
N1−H3A···O6	2.858(2)	1.85	172.5	*x*, 3/2 − *y*, 1/2 + *z*
N1−H4A···O5	2.961(2)	1.97	164.1	−1 + *x*, *y*, *z*
C2−H2···O1	2.893(2)	2.48	101.0	[a]
C9−H9···O4	2.903(2)	2.49	101.0	[a]
C21−H21···O1	3.180(2)	2.21	146.5	1 + *x*, 3/2 − *y*, −1/2 + *z*
C23−H23···O4	3.324(2)	2.44	137.3	1 + *x*, *y*, *z*
		FUROS−BPNO-H_2O (1:1:0.25)		
N1−H1A···O6	2.897(2)	2.04	140.2	−2 + *x*, *y*, 1 + *z*
N1−H1B···O2	2.886(2)	1.95	153.2	−1 − *x*, 1 − *y*, 2 − *z*
N2−H2···O3	2.698(2)	1.91	132.3	[a]
O4−H4···O6	2.564(2)	1.62	157.9	2 − *x*, 2 − *y*, 1 − *z*
C3−H3···O1	2.819(2)	2.35	104.1	[a]
C3−H3···O2	3.197(2)	2.46	124.0	−*x*, 1 − *y*, 2 − *z*
C11−H11···O3	3.239(2)	2.24	151.7	1 − *x*, 2 − *y*, 1 − *z*
C12−H12···O7	3.239(3)	2.22	154.1	*x*, 1 + *y*, *z*
C16−H16···O1	3.178(2)	2.11	165.5	1 + *x*, *y*, −1 + *z*
C18−H18···Cl1	3.703(2)	2.66	160.7	−*x*, 1 − *y*, 1 − *z*
C19−H19···O1	3.330(2)	2.31	155.2	1 + *x*, *y*, −1 + *z*
C22−H22···O7	3.256(3)	2.23	156.7	1 − *x*, 1 − *y*, 1 − *z*
		FUROS−INICNO (1:1)		
N2−H2A···O3	2.866(2)	1.87	167.1	−2 + *x*, *y*, *z*
N2−H2B···N4	3.074(2)	2.12	156.1	*x*, −1 + *y*, *z*
N3−H3A···O3	2.694(2)	1.87	135.7	[a]
N4−H4A···O1	2.784(2)	1.80	162.4	1 − *x*, 2 − *y*, −*z*
O4−H4C···O2	2.569(2)	1.60	167.7	2 + *x*, *y*, *z*
C4−H4···O5	3.277 (2)	2.35	142.0	*x*, −1 + *y*, *z*
C5−H5···O1	3.414(2)	2.33	176.5	2 − *x*, 1 − *y*, −*z*
C12−H12···O5	2.828(2)	2.36	103.8	[a]

[a] Intramolecular hydrogen bond.

50−70 cm^{-1} were clearly noted in the cocrystals due to the weakening of the N−H bond. A summary of the major overtone bands are listed in Table S3 in the Supporting Information.

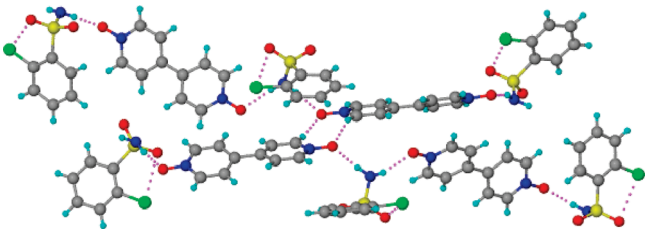

Figure 1. 2-CBS and BPNO molecules are connected via a strong N−H···O_{Noxide} hydrogen bond and such binary units extend via a dimeric C−H···O_{Noxide} motif.

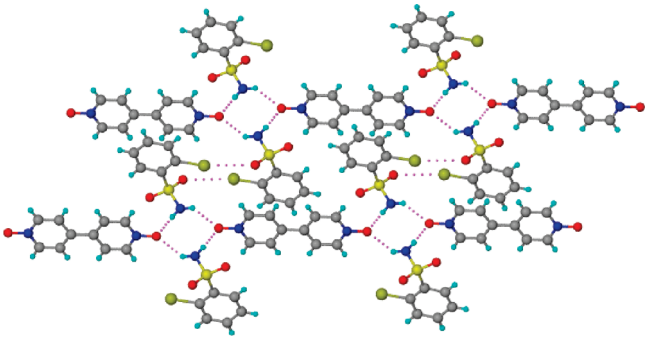

Figure 2. Tetrameric $R_4^2(8)$of N−H···O_{Noxide} hydrogen bonds ring motifs assemble the binary adduct.

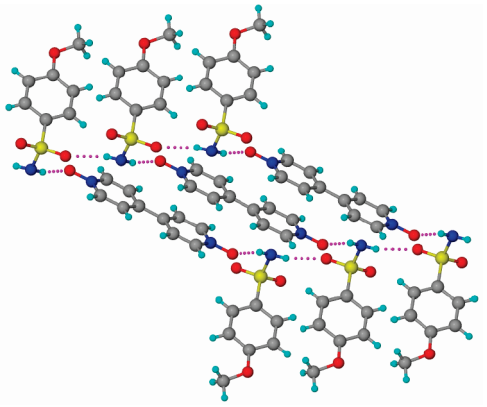

Figure 3. Hydrogen-bonded macrocyclic rings sustain the layer structure motif of 4-MBS−BPNO. A part of this crystal structure in the space group $P2_1/c$ may be discerned to contain a helix made up of N−H···O and C−H···O interactions along [001] (see Figure 4).

DISCUSSION

The formation of the sulfonamide−pyridine-N-oxide heterosynthon appears to be very reliable due to the enhanced hydrogen bond donor and acceptor ability of the sulfonamide NH and N-oxide, respectively. The formation of the dominant N−H···$O_{N\text{-}oxide}$ hydrogen bond in the crystal structure is based on the strongest donor (sulfonamide NH) interacting with the strongest acceptor (N-oxide).[6] The exact geometry of the sulfonamide motif, i.e., discrete N−H···O (D), infinite chain C(4), cyclic motifs $R_4^2(8)$ or $R_2^2(4)$ varies from one structure to another and it is difficult to anticipate their presence in a particular structure. Surprisingly, the two-point N−H···O + C−H···O heterosynthon of $R_2^2(8)$ geometry, similar to the carboxamide−pyridine-N-oxide heterosynthon was not observed in any

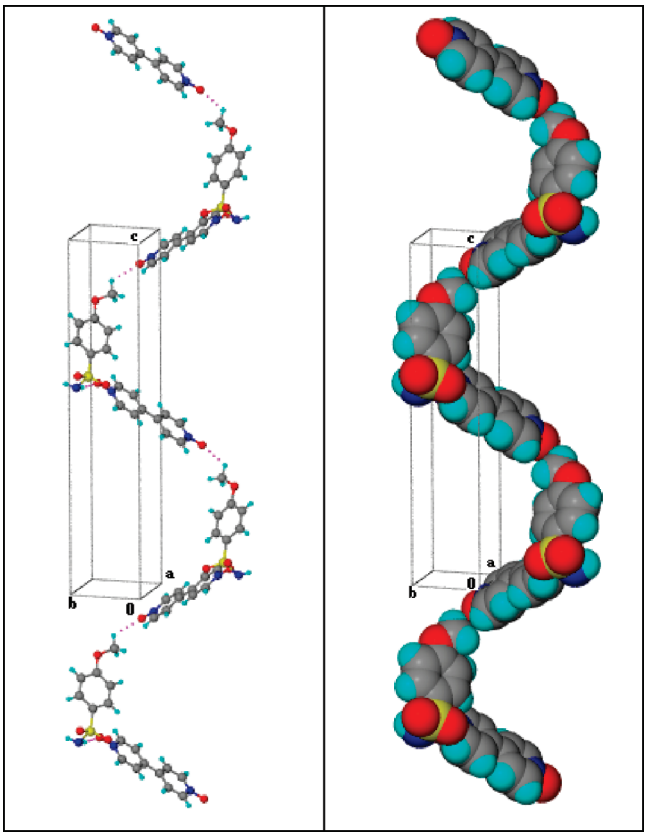

Figure 4. Helix formation through alternating 4-MBS and BPNO molecules.

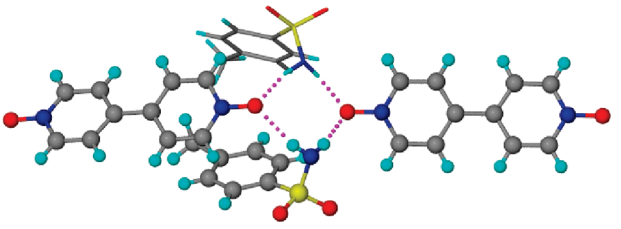

Figure 5. Tetrameric $R_4^2(8)$ rings of N−H···O hydrogen bonds between PTS and BPNO molecules. Symmetry-independent PTS molecules are shown as capped-stick and ball-stick models.

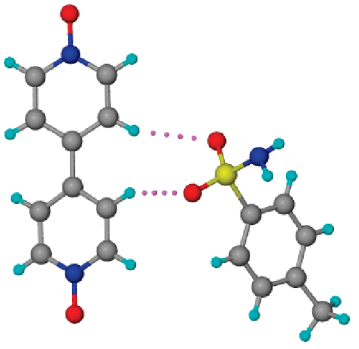

Figure 6. C−H···O synthon of $R_2^2(9)$ motif in the crystal structure.

structure. The nonplanarity of the SO_2NH_2 group compared to the planar $CONH_2$ perhaps prevents the two-point motif

dx.doi.org/10.1021/cg200094x |*Cryst. Growth Des.* 2011, 11, 1930–1939

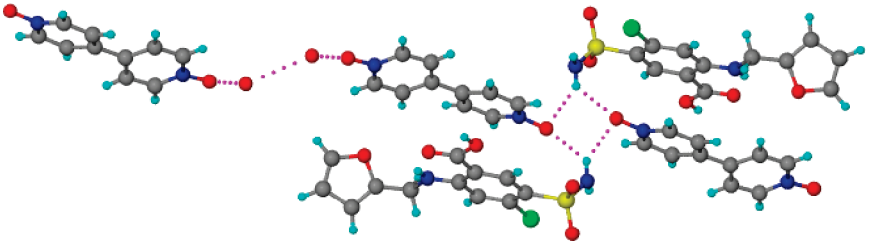

Figure 7. BPNO molecules are connected to FUROS through tetrameric $R_2^2(4)$ ring motif on one side (right) and to another BPNO molecule through water bridges on the other side (left).

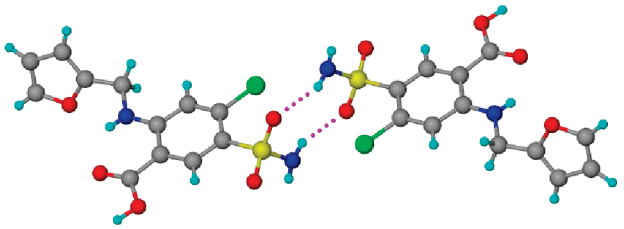

Figure 8. FUROS molecules connected through strong sulfonamide dimer $R_2^2(8)$ motif.

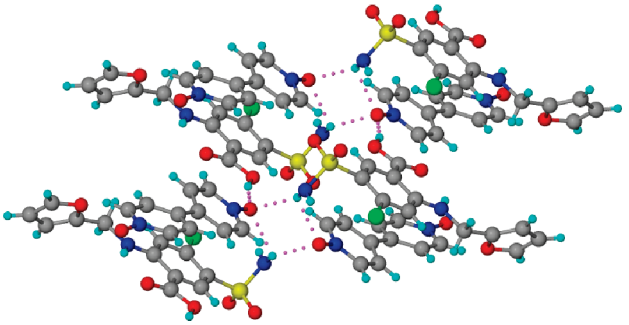

Figure 9. Tetrameric $R_2^2(4)$ ring motifs are connected through O−H···O_{Noxide} hydrogen bond.

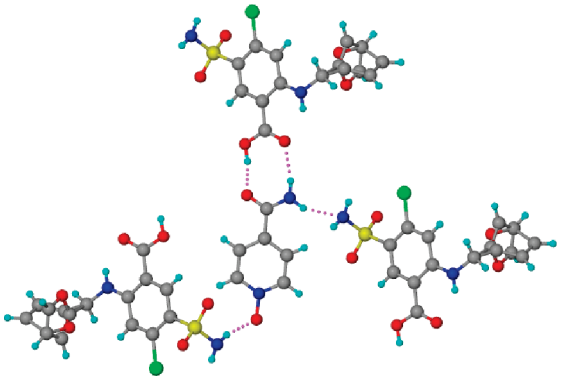

Figure 10. INICNO coformer is connected to FUROS by amide−acid $R_2^2(8)$ motif and N−H···N hydrogen bond.

with an aromatic partner group. Whereas the six heavy atoms in the SO_2NH_2 dimer adopt the chair cyclohexane conformation, the arrangement is planar in the amide dimer. Even though a dominant sulfonamide−pyridine-N-oxide motif could not be identified in this subset of cocrystal structures, it is clear that bimolecular recognition can be reproducibly

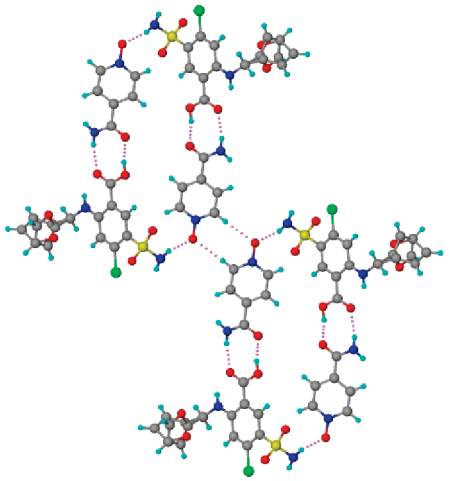

Figure 11. $R_4^4(32)$ $[R_2^2(8)]$ motif of N−H···O and O−H···O hydrogen bonds and C−H···O $R_2^2(8)$ dimer in FUROS−INICNO structure.

mediated between molecules (say drug and coformer) containing these two functional groups via a N−H···O_{Noxide} hydrogen bond or ring motif. A second preliminary observation is the lack of polymorphism in the cocrystals studied (based on the crystallization experiments listed in Table S4 in the Supporting Information), compared to relatively promiscuous multiple forms in some sulfonamides studied by us recently,[22] and for sulfa drugs in general.[12]

The newly identified sulfonamide−N-oxide heterosynthon is illustrated with the loop diuretic Furosemide.[23] The recurring sulfonamide N−H···O $R_2^2(8)$ dimer in three polymorphs of this drug[24] is present in the hydrate with BPNO. The anti NH makes an $R_2^2(4)$ ring motif with the N-oxide. The situation in FUROS−INICNO cocrystal is quite predictable: the strongest SO_2NH_2 donor bonds to the N-oxide acceptor, and the COOH and $CONH_2$ groups of the drug and coformer make the acid−amide heterosynthon at the next level of hierarchy.

CONCLUSIONS

The ability of aromatic primary sulfonamides to make a strong hydrogen bond with pyridine-N-oxides is demonstrated for the first time and then this synthon is used to make cocrystals of the loop diuretic drug Furosemide. The scope of this model study will be easily extendable to sulfa drugs. The fact that pyridine-N-oxide functional group is present in some drug molecules and discovery candidates[25] leads to the possibility of making two-drug cocrystals.

Table 3. Summary of Experimental Conditions and Results

S. no.	experimental conditions	product obtained
1	2-chlorobenzene sulfonamide (2-CBS) (0.1 mmol) + Bipyridine-N,N'-dioxide BPNO (0.1 mmol)	
	MeOH, 4 mL, room temperature (RT), solution crystallization (SC)	no cocrystal observed
	EtOH, 4 mL, RT, SC	no cocrystal observed
	i-PrOH, 4 mL, RT, SC	BPNO hydrate
	n-PrOH, 4 mL, RT, SC	1:1 cocrystal after 4−5 d
2	2 bromobenzene sulfonamide (2-BBS) (0.1 mmol) + bipyridine-N,N'-dioxide BPNO (0.1 mmol)	
	MeOH, RT, 3 mL, SC	no cocrystal observed
	EtOH, RT, 4 mL, SC	1:0.5 cocrystal after 2−3 d
	n-PrOH, RT, 4 mL, SC	BPNO hydrate
	DMF, RT, 3 mL, SC	no cocrystal observed
3	4-methoxybenzene sulfonamide (4-MBS) (0.1 mmol) + bipyridine-N,N'-dioxide BPNO (0.1 mmol)	
	MeOH, RT, 4 mL, SC	BPNO hydrate
	EtOH, RT, 4 mL, SC	4-MBS crystals
	i-PrOH, RT, 5 mL, SC	4-MBS crystals
	n-PrOH, RT, 4 mL, SC	1:0.5 cocrystal after 4−5 d
	DMF, RT, 3 mL,SC	no cocrystal observed
	DMSO, RT, 3 mL, SC	no cocrystal observed
4	*p*-toluene sulfonamide (PTS) (0.1 mmol) + bipyridine-N,N'-dioxide BPNO (0.1 mmol)	
	MeOH, 5 mL, RT, SC	no cocrystal observed
	EtOH, 5 mL, RT, SC	no cocrystal observed
	n-PrOH, 4 mL, RT, SC	PTS
	i-buOH, 7 mL, RT, SC	2:1 cocrystal after 4−5 d
5	furosemide (FUROS) (0.1 mmol) + bipyridine-N,N'-dioxide (BPNO) (0.1 mmol)	
	MeOH, 9 mL, RT, SC	FUROS Form 1
	Abs. EtOH, 6 mL, RT, SC	BPNO hydrate
	DMSO, 3 mL, RT, SC	no cocrystal observed
	DMF, 3 mL, RT, SC	no cocrystal observed
	4−5 drops CH_3CN, liquid-assisted grinding (LAG)	1:1:0.25 hydrate after 4 d
	MeOH, 9 mL, RT, SC	
	4−5 drops CH_3CN, LAG	FUROS Form 1
	EtOH, 6 mL, SC, RT	
	4−5 drops CH_3CN, LAG	no cocrystal observed
	i-PrOH, 6 mL, RT, SC	
	4−5 drops CH_3CN, LAG	FUROS Form 1
	n-PrOH, 6 mL, RT, SC	
6	furosemide (FUROS) (0.1 mmol) + Isonicotinamide N-oxide (INICNO) (0.1 mmol)	
	4−5 drops CH_3CN, LAG	no cocrystal observed
	MeOH, 6 mL, RT, SC	
	4−5 drops CH_3CN, LAG	1:1 cocrystal after 4 d
	EtOH, 6 mL, RT, SC	
	4−5drops CH_3CN, LAG	no cocrystal observed
	n-PrOH, 5 mL, RT, SC	
	4−5 drops CH_3CN, LAG	no cocrystal observed
	i-PrOH, 6 mL, RT, SC	
	4−5 drops CH_3CN, LAG	no cocrystal observed
	i-BuOH, 6 mL, RT, SC	
	4−5 drops CH_3CN, LAG	no cocrystal observed
	n-BuOH, 6 mL, RT, SC	

dx.doi.org/10.1021/cg200094x |*Cryst. Growth Des.* 2011, 11, 1930–1939

Table 4. IR Stretching Frequencies of N−H Group in Cocrystal Compared to the Starting Sulfonamide

primary sulfonamide N−H stretch		N−H stretch in N-oxide cocrystal	
FUROS	3400.0, 3351.0	FUROS−BPNO	3392.7, 3326.0
2-BBS	3364.3, 3261.0	2-BBS−BPNO	3286.6, 3194.2
4-MBS	3347.2, 3270.1	4-MBS−BPNO	3297.2
2-CBS	3356.0, 3254.0	2-CBS−BPNO	3332.7, 3240.3
PTS	3325.7, 3243.0	PTS−BPNO	3290.0, 3238.1
FUROS	3400.0, 3351.0	FUROS−INICNO	3390.2, 3316.1

EXPERIMENTAL SECTION

Cocrystal Preparation. Starting materials were purchased from commercial suppliers. Pyridine N-oxides were prepared by the oxidation of the corresponding pyridines with m-CPBA. The crystallization scale, number of experiments carried out, and the conditions used are summarized in Table 3. A full list of experiments, crystallization conditions and results are given in Table S4 (Supporting Information). Broadly, two methods were adopted: (1) the components were dissolved in a suitable solvent and crystallization of new crystals was examined, and (2) the components were ground with a few drops of solvent added, and then the material was dissolved in a solvent for single crystals to appear. The formation of a new crystalline phase was monitored by changes in sulfonamide NH IR bands from starting material to the product cocrystal followed by diffraction and spectroscopic confirmation as shown in Table 4.

X-ray Crystal Structure. Reflections were collected on a Bruker SMART APEX-CCD diffractometer. Mo−Kα (λ = 0.71073 Å) radiation was used to collect X-ray reflections on the single crystal. Data reduction was performed using Bruker SAINT software.[26] Intensities for absorption were corrected using SADABS.[27] RLATT3 and CELL_NOW programs[28] were used to generate a new reindexed cell for the structure MBS−BPNO, which was used during initialization and merging of raw data. Crystal structures were solved by direct methods and refined on F^2 with SHELXS-97 and SHELXL-97 programs[29] to give satisfactory R factor. Hydrogen atoms on O and N were experimentally located in difference electron density maps. All C−H atoms were fixed geometrically using HFIX command in SHELX-TL. In the modeled structure FUROS−INICNO the disorder was modeled for all the heavy atoms with isotropic displacement parameters using the PART command by assigning sof (site occupancy factor) of 0.5 and 0.5 for the two parts using the FVAR command. A check of the final CIF file using PLATON[30] did not show any missed symmetry. X-Seed[31] was used to prepare packing diagrams.

Vibrational Spectroscopy. Nicolet 6700 FT-IR spectrometer with a NXR FT-Raman and NIR Module was used to record IR and Raman and NIR spectra. IR and NIR spectra were recorded on samples dispersed in KBr pellets. Raman spectra were recorded on samples contained in standard NMR diameter tubes or on compressed samples contained in a gold-coated sample holder.

Thermogravimetric Analysis. TGA was performed on a Mettler Toledo TGA/SDTA 851e module. The sample 8−12 mg was placed in open alumina pan and the temperature increased from 30 to 400 °C at heating rate of 5 °C/min. The sample was purged by a stream of dry nitrogen at flow rate of 50 mL/min.

ASSOCIATED CONTENT

Supporting Information. IR, NIR, and Raman spectra; table of crystallization experiments; TGA curve (PDF); crystallographic CIF files. This material is available free of charge via the Internet at http://pubs.acs.org.

AUTHOR INFORMATION

Corresponding Author
*E-mail: ashwini.nangia@gmail.com.

ACKNOWLEDGMENT

N.R.G. and N.J.B. thank the CSIR and UGC for fellowship. We thank the DST (SR/S1/RFOC-01/2007 and SR/S1/OC-67/2006) and CSIR (01(2079)/06/EMRII) for research funding, and DST (IRPHA) and UGC (PURSE grant) for instrumentation and infrastructure facilities.

REFERENCES

(1) Desiraju, G. R. *Angew. Chem., Int. Ed.* **1995**, *34*, 2311.
(2) Walsh, R. D. B.; Bradner, M. W.; Fleischman, S. G.; Morales, L. A.; Moulton, B.; Rodriguez-Hornedo, N.; Zaworotko, M. J. *Chem. Commun.* **2003**, 186.
(3) Allen, F. H.; Motherwell, W. D. S.; Raithby, P. R.; Shields, G. P.; Taylor, R. *New. J. Chem.* **1999**, *23*, 25.
(4) Cambridge Crystallographic Data Center, Cambridge, U.K., www.ccdc.cam.ac.uk.
(5) (a) Nangia, A.; Desiraju, G. R. *Top. Curr. Chem.* **1998**, *198*, 57. (b) Nangia, A.; Desiraju, G. R. *Acta Crystallogr., Sect. A* **1998**, *54*, 934.
(6) (a) Etter, M. C.; Macdonald, J. C.; Bernstein, J. *Acta Crystallogr., Sect. B* **1990**, *46*, 256. (b) Bernstein, J.; Davis, R. E.; Shimoni, L.; Chang, N. L. *Angew. Chem., Int. Ed.* **1995**, *34*, 1555.
(7) (a) Etter, M. C. *J. Phys. Chem.* **1991**, *95*, 4601. (b) Etter, M. C. *Acc. Chem. Res.* **1990**, *23*, 120.
(8) (a) Fleischman, S. G.; Kuduva, S. S.; McMahon, J. A.; Moulton, B.; Walsh, R. D. B.; Rodriguez-Hornedo, N.; Zaworotko, M. J. *Cryst. Growth Des.* **2003**, *3*, 909. (b) Vishweshwar, P.; McMahon, J. A.; Bis, J. A.; Zaworotko, M. J. *J. Pharm. Sci.* **2006**, *95*, 499.
(9) (a) Bhogala, B. R.; Vishweshwar, P.; Nangia, A. *Cryst. Growth Des.* **2002**, *2*, 325. (b) Almarsson, Ö.; Zaworotko, M. J. *Chem. Commun.* **2004**, 1889. (c) Aakeröy, C. B.; Salmon, D. J. *CrystEngComm* **2005**, *7*, 439. (d) Bhogala, B. R.; Nangia, A. *New J. Chem.* **2008**, *32*, 800. (e) Aakeröy, C. B.; Beatty, A. M.; Helfrich, B. A. *Angew. Chem., Int. Ed.* **2001**, *40*, 3240.
(10) (a) Reddy, L. S.; Babu, N. J.; Nangia, A. *Chem. Commun.* **2006**, 1369. (b) Babu, N. J.; Reddy, L. S.; Nangia, A. *Mol. Pharmaceutics* **2007**, *4*, 417. (c) Babu, N. J.; Reddy, L. S.; Aitipamula, S.; Nangia, A. *Chem. − An Asian J.* **2008**, *3*, 1122.
(11) Nangia, A. *J. Chem. Sci.* **2010**, *122*, 295.
(12) (a) Yang, S. S.; Guillory, J. K. *J. Pharm. Sci.* **1972**, *61*, 26. (b) Ko, S.-K.; Jin, H. J.; Jung, D.-W.; Tian, X.; Shin, I. *Angew. Chem., Int. Ed.* **2009**, *48*, 7809. (c) Caira, M. R. *Mol. Pharmaceutics* **2007**, *4*, 310. (d) Byrn, S. R.; Pfeiffer, R. R.; Stowell, J. G. *Solid-State Chemistry of Drugs*; SSCI, Inc.: West Lafayette, IN, 1999; p 160.
(13) (a) Ishida, T.; In, Y.; Doi, M.; Inoue, M.; Yanagisawa, I. *Acta Crystallogr., Sect. B* **1989**, *45*, 505. (b) Leger, J. M.; Alberola, S.; Carpy, A. *Acta Crystallogr.* **1977**, *B33*, 1455. (c) Alberola, S.; Sabon, F.; Jaud et, J.; Galy, J. *Acta Crystallogr.* **1977**, *B33*, 3337. (d) Caira, M. R. *J. Chem. Crystallogr.* **1994**, *24*, 695. (e) Caira, M. R.; Nassimbeni, L. R.; Wilderwanck, A. F. *J. Chem. Soc., Perkin Trans.* **1995**, *2*, 2213. (f) Caira, M. R. *J. Crystallogr. Spectrosc. Res.* **1992**, *22*, 193.
(14) Eccles, K. S.; Elcoate, C. J.; Stokes, S. P.; Maguire, A. R.; Lawrence, S. E. *Cryst. Growth Des.* **2010**, *10*, 4243.
(15) (a) Reddy, L. S.; Basavoju, S.; Vangala, V. R.; Nangia, A. *Cryst. Growth Des.* **2006**, *6*, 161. (b) Videnova-Adrabińska, V.; Janeczko, E. *Chem. Commun.* **1999**, 1527. (c) Custelcean, R.; Moyer, B. A.; Bryantsev, V. S.; Hay, B. P. *Cryst. Growth Des.* **2006**, *6*, 555. (d) Custelcean, R.

Chem. Commun. **2008**, 295. (e) Custelcean, R.; Sellin, B.; Moyer, B. A. *Chem. Commun.* **2007**, 1541.

(16) (a) Shan, N.; Toda, F.; Jones, W. *Chem. Commun.* **2002**, 2372. (b) Trask, A. V.; Jones, W. *Top. Curr. Chem.* **2005**, *254*, 131.

(17) (a) Trask, A. V.; Motherwell, W. D. S.; Jones, W. *Chem. Commun.* **2004**, 890. (b) Friščić, T.; Trask, A. V.; Jones, W.; Motherwell, W. D. S. *Angew. Chem., Int. Ed.* **2006**, *45*, 7546.

(18) Reddy, L. S.; Bhatt, P.; Banerjee, R.; Nangia, A.; Kruger, G. J. *Chem. Asian J.* **2007**, *2*, 505.

(19) (a) Berry, D. J.; Seaton, C. C.; Clegg, W.; Harrington, R. W.; Coles, S. J.; Horton, P. N.; Hursthouse, M. B.; Storey, R.; Jones, W.; Friščić, T.; Blagden, N. *Cryst. Growth Des.* **2008**, *8*, 1697. (b) Bettinetti, G.; Caira, M. R.; Callegari, A.; Merli, M.; Sorrenti, M.; Tadini, C. *J. Pharm. Sci.* **2000**, *89*, 478.

(20) (a) Saha, B. K.; Nangia, A.; Jaskólski, M. *CrystEngComm* **2005**, *7*, 355. (b) Thaimattam, R.; Sharma, C. V. K.; Clearfield, A.; Desiraju, G. R. *Cryst. Growth Des.* **2001**, *1*, 103.

(21) International Union of Crystallography, Chester, U.K., checkcif. iucr.org.

(22) Sanphui, P.; Sarma, B.; Nangia, A. *Cryst. Growth Des.* **2010**, *10*, 4550.

(23) (a) Friedman, P. A.; Berndt, W. O. In *Modern Pharmacology with Clinical Applications*, 5th ed.; Craig, C. R., Stitzel, R. E., Eds.; Little Brown & Company: Boston, 1997; pp 239−255. (b) Khan, M. G. *Encyclopedia of Heart Diseases*; Elsevier: New York, 2006.

(24) Babu, N. J.; Cherukuvada, S.; Thakuria, R.; Nangia, A. *Cryst. Growth Des.* **2010**, *10*, 1979.

(25) (a) Feng, S.; Yang, M.; Zhang, Z.; Wang, Z.; Hong, D.; Richter, H.; Benson, G. M.; Bleicher, B.; Grether, U.; Martin, R. E; Plancher, J.-M.; Kuhn, B.; Rudolph, M. G.; Chen, L. *Biorg. Med. Chem. Lett.* **2009**, *19*, 2595. (b) McKeown, S. R.; Hejmadi, M. V.; McIntyre, I. A.; McAleer, J. J.; Patterson, L. H. *Br. J. Cancer* **1995**, *72*, 76. (c) Nishida, C. R.; Lee, M.; Ortiz de Montellano, P. R. *Mol. Pharm.* **2010**, *78*, 497.

(26) *SAINT-Plus, version 6.45*; Bruker AXS: Madison, WI, 2003.

(27) Sheldrick, G. M. *SADABS, Program for Empirical Absorption Correction of Area Detector Data*; University of Göttingen: Göttingen, Germany, 1997.

(28) (a) *RLATT, Reciprocal Lattice Viewer, version 3.0*; Bruker AXS: Madison, WI, 2000. (b) Sheldrick, G. M. *CELL_NOW*; University of Göttingen: Göttingen, Germany, 2004.

(29) (a) *SMART (Version 5.625) and SHELX-TL (Version 6.12)*; Bruker-AXS: Madison, WI, 2000. (b) Sheldrick, G. M. *SHELXS-97and SHELXL-97*; University of Göttingen:, Göttingen, Germany, 1997.

(30) Spek, A. L. *PLATON: A Multipurpose Crystallographic Tool*; Utrecht University: Utrecht, The Netherlands, 2002. Spek, A. L. *J. Appl. Crystallogr.* **2003**, *36*, 7.

(31) Barbour, L. J. *X-Seed, Graphical Interface to SHELX-97 and POV-Ray*; University of Missouri−Columbia: Columbus, MO, 1999.